

## 2003 Annual SCEC report

### InSAR investigation of interseismic strain accumulation on faults in the Eastern California Shear Zone

Publications resulted from this project:

Fialko, Y., Evidence of fluid-filled upper crust from observations of post-seismic deformation due to the 1992 Mw7.3 Landers earthquake, *J. Geophys. Res.*, 109, doi:10.1029/2003JB002985, 2004

Fialko, Y., Probing the mechanical properties of seismically active crust with space geodesy: Study of the co-seismic deformation due to the 1992 Mw7.3 Landers (southern California) earthquake, *J. Geophys. Res.*, 109, doi:10.1029/2003JB002756, 2004

Fialko, Y., L. Rivera, and H. Kanamori, Estimate of differential stress in the upper crust from variations in topography and strike along the San Andreas fault, *Geophys. J. Int.*, 2004 (in press).

Fialko, Y., Observations of surface seformation following the 1992 M7.3 Landers earthquake, southern California: Robust test of the post-seismic relaxation models, *Eos, Trans. AGU*, 84, Suppl., p. F484, 2003.

Fialko, Y., The Big Bend and the strength of the San Andreas fault, 25th IUGG Conference on Mathematical Geophysics, Columbia Univ., New York, 2004.

Fialko, Y., Interseismic strain accumulation on faults in the Eastern California Shear Zone from a decade of InSAR measurements, Proc. Annual SCEC Meeting, Palm Springs, 2004.

We used the entire catalog of the ERS data collected over the Mojave desert to identify subtle deformation signals due to the post-seismic relaxation and secular tectonic loading (*Fialko*, 2004a,b) in the Eastern California Shear Zone. By stacking of multiple interferograms, we suppressed the atmospheric noise, and effectively pushed InSAR toward its theoretical detection limit of the line of sight (LOS) velocities of the order of millimeters per year (e.g., *Fialko and Simons*, 2001; *Peltzer et al.*, 2001). Figure 1 shows a mosaic of several radar swaths from the ERS satellites, with colors indicating average LOS velocities for the time period 1992-1999. The stacked InSAR data reveal several features of interest. The lobes of LOS velocities around the 1992 Landers rupture (*Fialko*, 2004a) most likely result from the poro-elastic rebound of the fluid-saturated upper crust (*Fialko*, 2004b; *Peltzer et al.*, 1998). The ground water migration is also responsible for the negative LOS anomaly around the Harper Lake (117.2°W, 35°N), representing ground subsidence. We found a number of lineated zones of high gradients in the LOS velocities that are correlated with the geologically mapped faults. In Figure 1 some of these zones are indicated by the across-fault profiles (straight solid lines).

Our analysis of independent InSAR data confirmed high (5-7 mm/yr) strain accumulation rates on the Blackwater fault (*Oskin and Iriondo*, 2004; *Peltzer et al.*, 2001). Figure 2 shows the satellite range changes along the Blackwater fault. If the observed LOS velocity variations across the fault are interpreted as indicating a predominantly horizontal motion due to the interseismic fault creep at depth, the localized nature of the LOS displacements seem to require an abnormally small depth to the brittle-ductile transition of the order of 3 km (Figure 2). The width of the enhanced strain zone may be smaller still, as some spatial “smearing” of the near-fault velocities occurs in the process of projecting the data from a finite area onto a profile (e.g., if the profile is not strictly

Figure 1: Interferometric stack from the ERS tracks 170, 399, and 127 over the Mojave desert. Colors denote the average LOS velocities (stacked LOS displacements divided by the total time span of all interferograms in the stack), in cm/yr (positive toward the satellite). Black wavy lines denote Quaternary faults (*Jennings, 1994*). Magenta boxes and black straight lines denote profiles across several identified zones of strain accumulation.

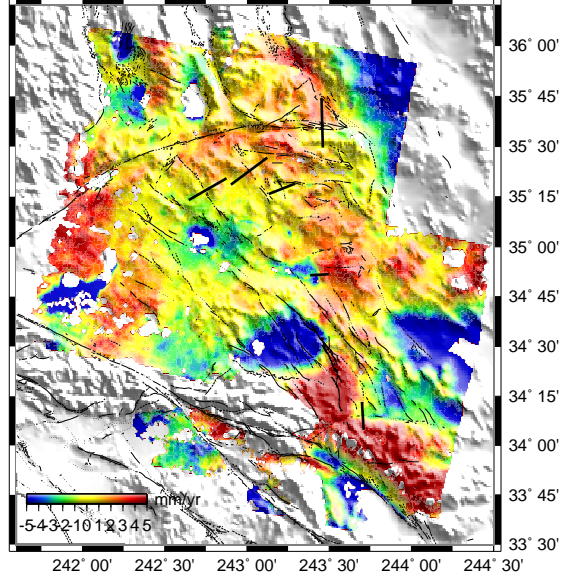
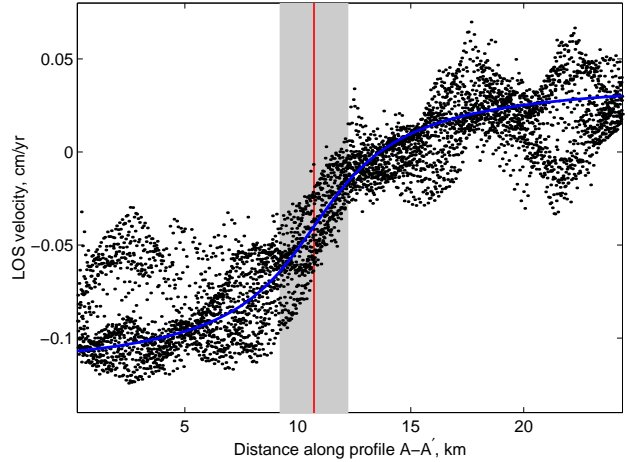


Figure 2: Variations in the satellite LOS velocities across the Blackwater fault. Black dots denote the stacked InSAR data from the 10 km wide swath collapsed onto profile A-A'. Red line shows the position of the fault trace. Blue line shows the predicted interseismic velocity assuming the locking depth of 3 km.



orthogonal to the fault, or if the fault has subtle variations in strike within the selected “data box”). Analysis of *Peltzer et al. (2001)* yielded a similar value of 5 km, which is likely an overestimate due to the same reason. Such a shallow transition from the locked seismogenic layer to the freely slipping fault is perhaps unrealistic. Our alternative hypothesis is that the interseismic strain accumulation on the Blackwater fault is due to a predominantly elastic deformation of the compliant fault zone surrounding the primary slip surface. Existence of wide (up to a few kilometers) zones of reduced elastic moduli around several faults in the Eastern California Shear Zone has been recently inferred from the analysis of InSAR data from the Hector Mine (*Fialko et al., 2002*) and Landers (*Fialko, 2004a*) earthquakes. According to the compliant fault zone model, the observed strain concentration on the Blackwater fault may represent a secular tectonic loading of a compliant fault zone that is  $\sim 3$  km wide (see gray shading around the geologically mapped fault position in Figure 2). Besides removing the need for an abnormally thin seismogenic layer, this interpretation may reconcile the short-term geodetic and the long-term geologic slip rates, and explain why the Blackwater fault does not offset the Garlock fault to the north. Furthermore, it may allow us to determine the rigidity

structure of the Blackwater fault, and the rate of fault stressing due to tectonic motion (provided that the rigidity structure of the fault zone is known). We performed detailed finite element simulations of the fault zone deformation to place some bounds on the range of the admissible fault properties (i.e., width of the compliant zone, the reduction in the effective elastic modulus, etc.), and quantify the model predictions (e.g., the rate of tectonic loading). A manuscript describing these results is in preparation.

While we find no evidence of the interseismic strain accumulation on the Garlock fault, except maybe the segment around  $116.8^{\circ}\text{W}$ ,  $35.6^{\circ}\text{N}$  (Figure 1), the Mule Spring/Leach Lake fault system (the easternmost extension of the Garlock fault) is expressed in a pronounced velocity gradient (Figure 1). However, the sign of the LOS velocity anomaly on the Mule Spring/Leach Lake faults is opposite to that expected of a pure strike slip, left-lateral deformation. Therefore it is likely that the observed strain accumulation on the Mule Spring/Leach Lake faults is due to vertical displacements (e.g., North side up, and/or South side down) across these faults, perhaps due to hydrologic processes, and/or dip-slip tectonics. A number of other faults in the Eastern California Shear Zone were found to be accumulating strain similar to the Blackwater fault system. For example, the stacked InSAR data revealed an on-going localization of strain on the Goldstone and Superior Lake faults to the east of the Blackwater fault (see profiles in Figure 1). In a follow-up project submitted to SCEC we propose to incorporate these observations into a large-scale model of fault systems in Southern California.

In a synergetic study, we investigated the relationships between major bends of the San Andreas fault in with variations in the along-fault topography (Fialko *et al.*, 2004). We demonstrated that the topography-induced perturbations in the intermediate principal stress may result in the fault rotation with respect to the maximum compression axis provided that the fault is non-vertical, and the slip is horizontal. The progressive fault rotation may produce additional topography via thrust faulting in the adjacent crust, resulting in a positive feedback. The inferred relationship between topography and fault orientation admit a simple physical interpretation. An increase in the vertical stress on a dipping fault introduces a component of normal faulting into the resolved shear stress on the fault. In order to maintain the strike slip, the fault must rotate to higher angles to the maximum compressive stress axis, thereby introducing a component of thrust faulting that will balance out the component of normal faulting introduced by the excess topography. We used the observed rotation of the fault plane due to the along-fault variations in topography to infer the magnitude of the in situ differential stress. Our results (see Figure 3) suggest that the average differential stress in the upper crust around the San Andreas fault is of the order of 50 MPa, implying the effective fault strength that is about a factor of two less than predictions based on the Byerlee's law and the assumption of hydrostatic pore pressures.

## References

- Fialko, Y., Probing the mechanical properties of seismically active crust with space geodesy: Study of the co-seismic deformation due to the 1992  $M_w$ 7.3 Landers (southern California) earthquake, *J. Geophys. Res.*, *109*, 10.1029/2003JB002,756, 2004a.
- Fialko, Y., Evidence of fluid-filled upper crust from observations of post-seismic deformation due to the 1992  $M_w$ 7.3 Landers earthquake, *J. Geophys. Res.*, *109*, 10.1029/2004JB002,985, 2004b.
- Fialko, Y., and M. Simons, Evidence for on-going inflation of the Socorro magma body, New Mexico, from Interferometric Synthetic Aperture Radar imaging, *Geophys. Res. Lett.*, *28*, 3549–3552, 2001.

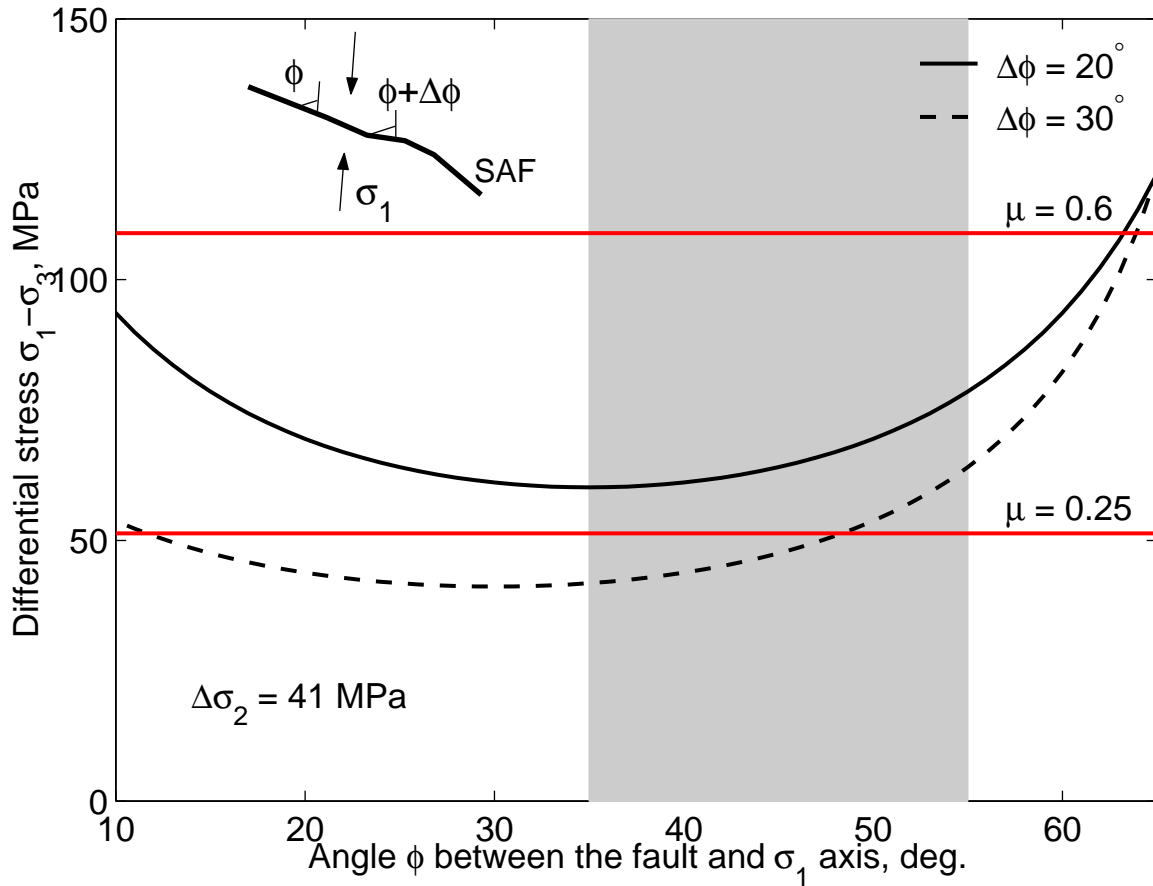


Figure 3: Dependence of the differential stress on angle  $\phi$  between the fault and the maximum compressive stress axis, for values of  $\Delta\phi$  spanning the likely range of the observed fault rotation. The shaded area indicates the range of  $\phi$  inferred from the inversions of the earthquake focal mechanisms (*Hardebeck and Hauksson, 1999*). Horizontal lines show the maximum average differential stress for different coefficients of friction  $\mu$ . The inset illustrates the geometry of the problem.

- Fialko, Y., D. Sandwell, D. Agnew, M. Simons, P. Shearer, and B. Minster, Deformation on nearby faults induced by the 1999 Hector Mine earthquake, *Science*, *297*, 1858–1862, 2002.
- Fialko, Y., L. Rivera, and H. Kanamori, Estimate of differential stress in the upper crust from variations in topography and strike along the San Andreas fault, *Geophys. J. Int.*, in press, 2004.
- Hardebeck, J. L., and E. Hauksson, Role of fluids in faulting inferred from stress field signatures, *Science*, *285*, 236–239, 1999.
- Jennings, C., *Fault activity map of California and adjacent areas, with locations and ages of recent volcanic eruptions*, California Division of Mines and Geology, Geologic Data Map No. 6, map scale 1:750,000, 1994.
- Oskin, M., and A. Iriondo, Large-magnitude transient strain accumulation on the Blackwater fault, Eastern California shear zone, *Geology*, *32*, 313–316, 2004.
- Peltzer, G., P. Rosen, F. Rogez, and K. Hudnut, Poroelastic rebound along the Landers 1992 earthquake surface rupture, *J. Geophys. Res.*, *103*, 30,131–30,145, 1998.
- Peltzer, G., F. Crampe, S. Hensley, and P. Rosen, Transient strain accumulation and fault interaction in the Eastern California shear zone, *Geology*, *29*, 975–978, 2001.